

Effect of double doping of CUO films with cadmium and cobalt eras on the structural and electrical properties

Nabeel khalil Husien ¹

¹ Department of Physics, College of Science, University of Diyala, Iraq

Email: sciphysics2122@uodiyala.edu.iq

J. Alzanganawee ^{1*}

¹ Department of Physics, College of Science, University of Diyala, Iraq

Email: sciphysics2122@uodiyala.edu.iq

ABSTRACT

In this study, CuO thin films were deposited from the preparation of a gelatinous solution of aqueous copper acetate at a concentration of 0.6 M dissolved in 2-methoxyethanol, and mono ethanolamine was added to neutralize the pH of the solution to reach (Ph =7)) on glass bases and double-grafted with cadmium and cobalt in equal proportions. [(1+1), (3+3), (5+5), and(7+7)]. The roughness of the as-prepared pure and double-grafted films (Cd, Co) was studied using atomic force microscopy (AFM). Using the Hall effect measurement, the p-type to n-type conductivity was determined, and finally a lower resistance was found at the grafting ratio (5+5) ($2.86 \times 10^{-2} (\Omega \cdot \text{m})$) above results depict that (5+5) wt.% of thin films doped may have potential application in the field of optoelectronic devices.

Keywords:

aqueous copper acetate, cadmium acetate, cobalt acetate, sol-gel method, technique, perm coating, annealing, study of the effect of grafting.

1-Introduction

Copper oxides are gaining newfound attention as potentially useful TCO materials for use in the production of a wide variety of optoelectronic devices. Copper oxide is an attractive substance since it is non-toxic, inexpensive, and abundantly available, and the synthesis of copper oxide is quite straightforward. [1]. CuO (monoclinic) demonstrates p-type conductivity and is a semiconductor with a band gap of(1.9 – 2.1 eV), which is near to the ideal band gap that is utilized for the absorber layer in solar cells. [2-4]. and because of the existence of copper vacancies in its structure In few recent decades, more scientists focused their interest on the performance of some material properties to develop the characteristics of

reliable gas sensors due to their wide applications and great diversity in many sectors, such as home safety, chemical controlling, industrial monitoring, and other hazardous environmental sensing applications[5]. Because of the changes in conductivity that are brought on by the reaction of gases with surface-adsorbed oxygen, CuO has been used in heterogeneous catalysis for a number of environmental processes, as well as in the production of gas sensing devices. This is because CuO has a high solubility in oxygen. It has demonstrated that it is one of the promising options to replace the hazardous and costly materials such as ZnO, SnO₂, In₂O₃, and others like them for possible applications such as dye-sensitized solar cells.[6]. batteries using lithium ion, electro

chromic coatings, applications using catalytic reactions, and gas sensors [1]. The physical properties of CuO have been adjusted by the suitable dopants in order to create a device that is useful. [7, 8]. Pulsed laser deposition is one of the many ways that have been utilized to effectively manufacture CuO. [9], spin-coating [10], thermal evaporation [11], combustion caused by microwaves, chemical vapor deposition, and microwave ovens [12]. The spin coating process is one of the most successful approaches to the manufacture of transition metal oxide films among these several procedures. The spin coating technology has many benefits, including the ability to control the rate of deposition, the formation of oriented crystalline layers, and more. Using the spin coating method, we provide in this article a straightforward method for producing Co-doped CuO thin films by deposition onto a soda lime glass substrate from solutions containing varying concentrations of Cd and Co. The deposition process is carried out from the solutions. Investigations were carried out on the We looked into the surface appearance and crystalline structure of both un-doped and Co-doped CuO films. It was determined by hall effect measurements.. atomic force microscopy (AFM) was utilized to provide information on the crystalline nature and surface morphology of the thin film samples, and scanning electron microscopy (SEM) was employed to disclose the electrical properties of the films.

2- Experimental details

Pure copper acetate, also known as $\text{Cu}(\text{CH}_3\text{COO})_2 \cdot \text{H}_2\text{O}$, was the copper precursor solution that was initially dissolved in 2-methoxyethanol to produce a 0.6 M solution. This solution was then agitated using a magnetic stirrer for twenty minutes at a temperature of twenty-seven degrees Celsius in order to ensure that the necessary concentrations of solutions were obtained. Pure copper must be used in order to achieve the desired levels of solution concentration (II) In order to prepare the (Cd + Co) co-loaded mixtures, 0.6 M of copper acetate di-hydrate ($\text{Cu}(\text{CH}_3\text{COO})_2 \cdot 2\text{H}_2\text{O}$), cobalt acetate, and

cobalt chloride were combined. ($\text{Co}(\text{CH}_3\text{COO})_2 \cdot 2\text{H}_2\text{O}$) and cadmium acetate dihydrate ($\text{Cd}(\text{CH}_3\text{CO}_2) \cdot 2\text{H}_2\text{O}$) were dissolved in 2-methoxyethanol and then combined together in order to obtain (1+1), (3+3), (5+5), and (7+7) wt percent (Cd + Co) co-loaded CuO. The mixes were then mixed for a total of twenty minutes at a temperature of twenty-seven degrees Celsius. After the temperature of the plate was brought up to 75 degrees Celsius in a measured manner, the stabilizing agent mono ethanolamine was added to the solutions in a measured fashion. After stirring for a total of 1:30 hours, the resulting solutions and combinations were brought to a homogenous state. The glass substrates were cleaned in a sequence consisting of acetone, ethanol, and deionized water prior to the deposition process. After being coated onto glass substrates at a speed of 3300 rpm for 40 seconds, each and every CuO thin film was instantly dried on a hot plate at a temperature of 200 degrees Celsius. This process was performed three more times, and then the samples were annealed at a temperature of 475 degrees Celsius for one hour while being exposed to air. Through the use of atomic force microscopy, the structural features of the films that were deposited were investigated (AFM, Park XE-100, Park Systems). The Hall Effect measurement equipment (ECOPIA HMS-5000, USA) and the four point probe method are utilized in order to get an accurate reading of the electrical characteristics. The resistance was measured at a temperature of 200 K in the presence of air and NO_2 gas environment using an Agilent 34,401 A digital multimeter that included an in-built source of constant voltage power supply. The gas response (S) of NH_3 can be described as $S = 14(R_a R_g) / R_a$, where R_g and R_a are the CuO film resistances that are measured in the NH_3 and air atmospheres, respectively. The specifics of the gas exposure and the method of measurement have been disclosed elsewhere. [13].

3-Results and discussion

The grain size (Average Grain), the average surface roughness (Average Roughness), and the square root rate (RMS Roughness) were all

calculated through the use of atomic force microscopy, which was used to study the surface topography and surface crystal structure of the precipitated films. RMS Roughness represents the square of the sum of the heights and depressions of the grains over their sum. Average Grain represents the average grain size. Average Roughness represents the average surface roughness. Below the square root, the surface will be more regular and have less roughness if the value of the square root average is smaller. Figure (1) shows the two-dimensional and three-dimensional AFM images of the distribution of grains on the surfaces of the prepared films, as it was in general semi-homogeneous, and the percentage of the homogeneity of the membrane varies according to the annealing temperature and the grafting ratios, as the two-dimensional (2D) and three-dimensional (3D) images showed spherical Nano shapes and Flowers and Cauli-Flowers, Table. (1) reveals the particle size as well as the surface roughness rate and the root square rate. It was

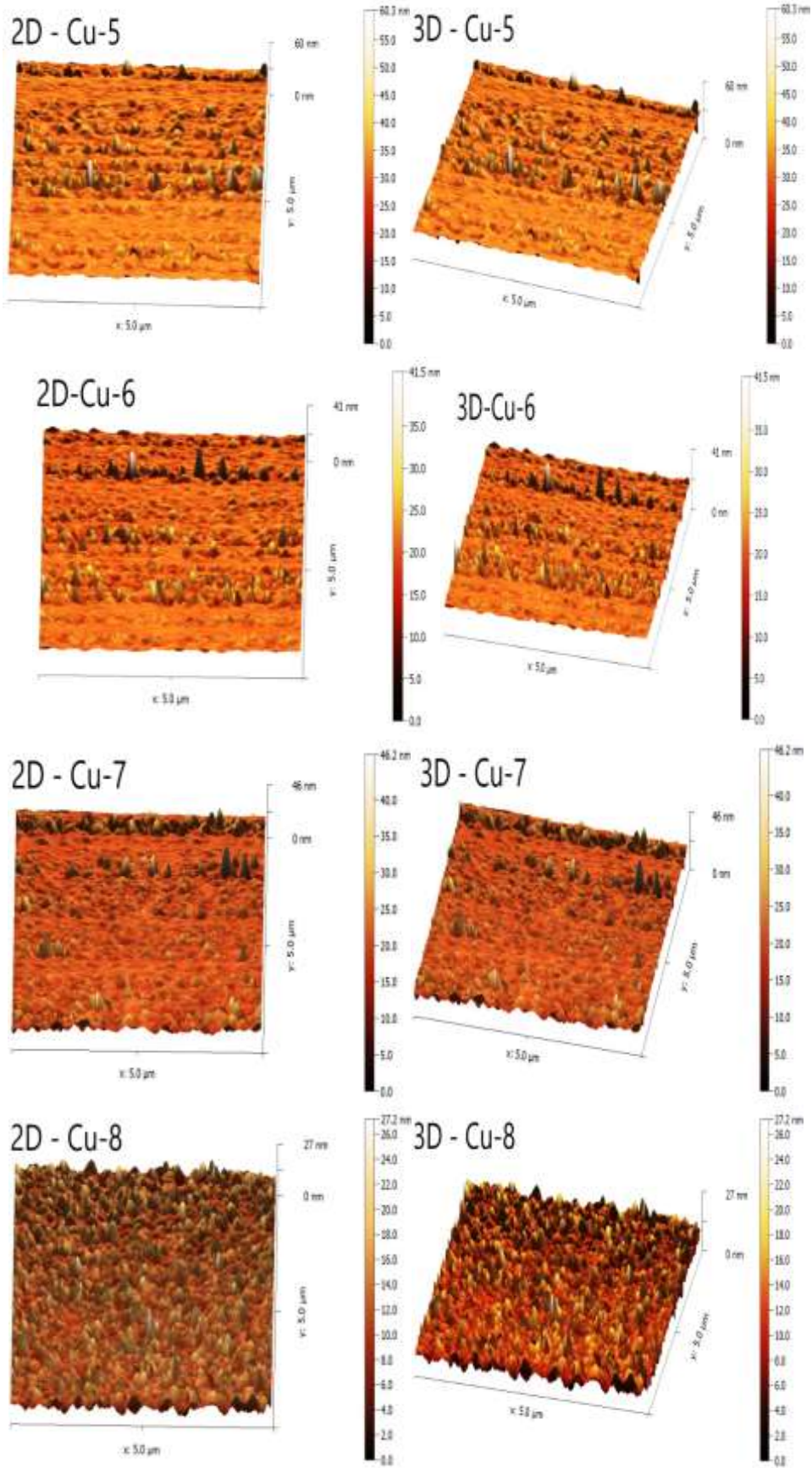
found that the CuO film dotted with the values of particle size and roughness rate gradually increased with increasing grafting ratios of the samples (Cu-5,Cu-6,Cu-7), and this indicates occupancy (Cd + Co) for inter-grain regions and inter-sites within the crystal lattice. This was discovered after it was found that the CuO film dotted with the values of particle size and roughness rate gradually increased with increasing grafting ratios of the samples[14, 15]. Figure (2b) illustrates the correlation between grain size and grafting ratios, while Figure (2a) demonstrates the correlation between roughness rate and grafting ratios. As for samples with high percentages (Cu-9), we see a reduction in the grain size and roughness, as shown in Figure (2b), and we believe that this reduction is most likely due to the occupancy of the grafting atoms compensatory sites for the CuO membrane lattice. The images that were obtained using the AFM are almost identical to those that were obtained by researchers in earlier studies. [15, 16]

Table (1) values of the surface roughness and the square root of the mean square of the roughness and particle size of the prepared films.

Sample Code	Average Roughness (nm)	RMS Roughness (nm)	Average Grain Size (nm)
Cu-5	1.69	2.72	30.25
Cu-6	1.22	1.88	19.94
Cu-7	1.63	2.33	20.18
Cu-8	1.85	2.39	11.17
Cu-9	1.26	2.03	26.12

It was also observed from the distribution of granular accumulation concentrations in Figure 2 that the values of the size of the particles fall within the Nano scale, with the diversity of crests creep towards the different granular sizes, depending on the ratios of co-

doping [(Cd + Co) co-doping]. The roughness rate represents the measure of surface quality, as the increase in An increase in the roughness rate can lead to scattering of the incident light and thus a decrease in optical transmittance



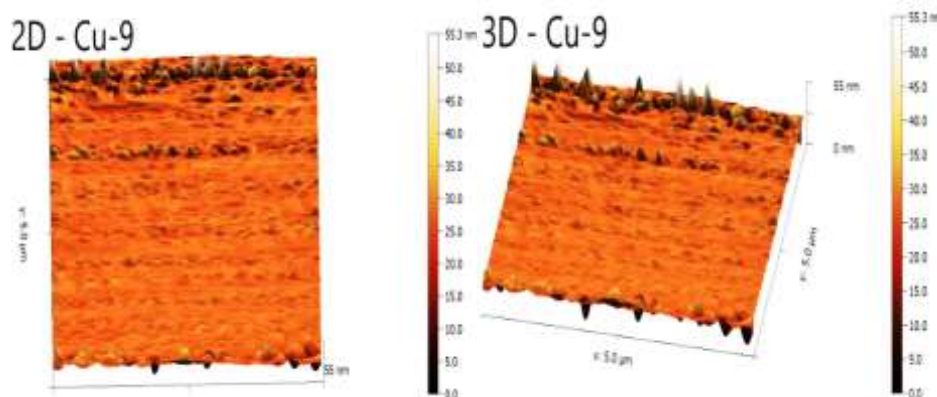


Figure 1. 2D and 3D AFM images of undoped and di-doped (CuO) films in equal proportions with cadmium and cobalt annealed at 475 °C.

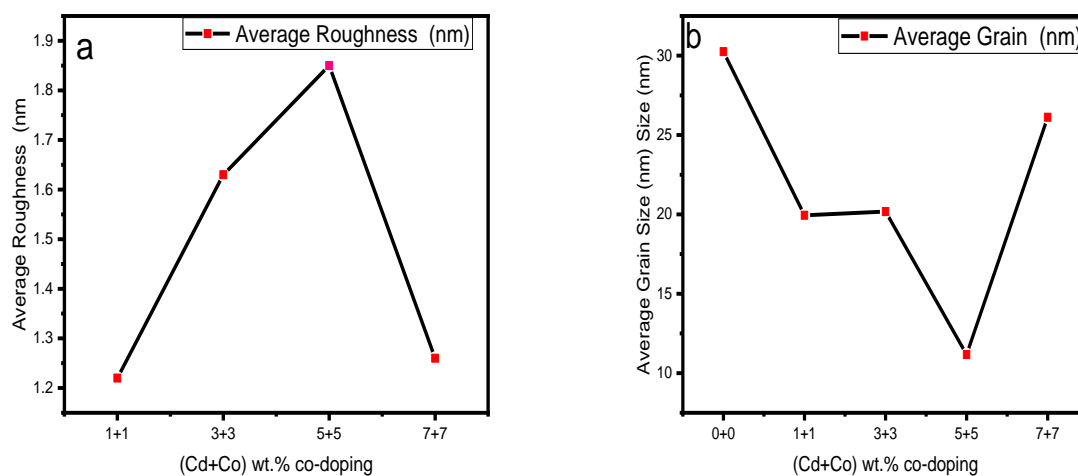


Figure (2)a: Roughness change(b): Granular size change with equal doping ratios of CuO . films

2- Electrical Measurements

To find out the electrical properties of un doped (CuO) thin films grafted with equal proportions of cadmium ions (Cd⁽⁺²⁾) and cobalt ions (Co⁽⁺²⁾) with an annealing degree (475 °C), Hall effect measurement was carried out. Each of the Hall coefficient (R_H) and the concentration of carriers [Carrier Concentration (n)] and electrical conductivity [Conductivity (σ)] [Resistivity (ρ)] mobility [Mobility (μ)] and as shown in Table (2) shows Results The positive sign of the results is Hall coefficient that the type of charge carriers is (p-type) the positive type (that is, the majority of charge carriers are the gaps) for ungrafted CuO films. The results also showed a change in charge carriers from (p-type) the positive type to (n-Type) the negative type as a result of an increase in the concentration of cadmium ions and cobalt ions in the CuO lattice, and we

notice an improvement in the electrical properties, as we notice an increase in the values of conductivity and charge carriers, and a decrease in the values of Hall's modulus and specific resistivity for the majority of CuO films grafted with equal proportions of cadmium ions and cobalt ions, and this indicates an increase Electron concentration by grafting with cadmium and cobalt into a Cu . lattice O reticulum, which stimulates electrical activation [17],as shown in Figure (3), or the reason may be due to the substitution of cadmium (Cd²⁺ions) and cobalt (Co²⁺ ions) for copper ions. (Cu²⁺ ions), which causes an increase in the crystal size that leads to disruption of the crystal lattice and then increases the oxygen spaces that increase the electrical conductivity [18], and from the results it was found at the ratio of grafting (5 + 5) and the ratio (7 + 7) The Hall modulus

increases and the conductivity and carrier concentration decrease. The reason for the decrease in carrier concentration may be the increase in the charge transfer reaction through collision in the lattice. The higher the carrier concentration and the lower the

mobility [19], as when the size of the particles or particles decreases or the strain of the network increases, the number of free carrier concentration decreases and thus the electrical resistance increases [20].

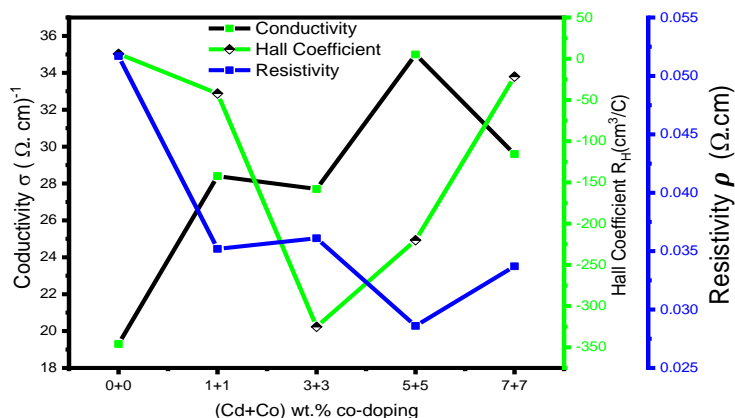


Figure 3. Electrical conductivity, specific resistance and Hall's modulus as a function of doping ratios of un doped CuO films doped with cadmium and cobalt annealed at (475 °C)

Table (2) Results of Hall effect measurements for un doped and doped CuO films with cadmium and cobalt

Sample Code	Conductivity σ ($\Omega.cm$) ⁻¹	Carrier Concentration n (cm) ⁻³	Resistivity ρ ($\Omega.cm$)	Mobility μ (cm^2/Vs)	Hall Coefficient R_H (cm^3/C)	Type
Cu-4	1.93E+01	1.04E+18	5.17E-02	1.16E+02	5.98E+00	P
Cu-5	2.84E+01	-1.48E+17	3.52E-02	1.20E+03	-4.22E+01	N
Cu-6	2.77E+01	-1.92E+16	3.61E-02	9.02E+03	-3.25E+02	N
Cu-7	3.50E+01	-2.83E+16	2.86E-02	7.71E+03	-2.20E+02	N
Cu-8	2.96E+01	-2.89E+17	3.37E-02	6.39E+02	-2.16E+01	N

References

[1] B. Boudjema, R. Daira, A. Kabir, and R. Djebien, "Physico-chemical properties of CuO thin films deposited by spray pyrolysis," in *Materials Science Forum*, 2017, vol. 895: Trans Tech Publ, pp. 33-36.

[2] S. C. Ray, "Preparation of copper oxide thin film by the sol-gel-like dip technique and study of their structural and optical properties," *Solar energy materials and solar cells*, vol. 68, no. 3-4, pp. 307-312, 2001.

[3] E. M. Alkoy and P. Kelly, "The structure and properties of copper oxide and copper aluminium oxide coatings prepared by pulsed magnetron sputtering of powder targets," *Vacuum*, vol. 79, no. 3-4, pp. 221-230, 2005.

[4] A. Amri *et al.*, "Surface structural features and optical analysis of nanostructured Cu-oxide thin film coatings coated via the sol-gel dip coating method," *Ceramics International*, vol. 45, no. 10, pp. 12888-12894, 2019.

[5] D. Jundale *et al.*, "Nanocrystalline CuO thin films for H2S monitoring:

- microstructural and optoelectronic characterization," *Journal of Sensor Technology*, vol. 1, no. 2, pp. 36-46, 2011.
- [6] S. J. Mezher, M. O. Dawood, O. M. Abdulmunem, and M. K. Mejbil, "Copper doped nickel oxide gas sensor," *Vacuum*, vol. 172, p. 109074, 2020.
- [7] S. Bahoosh, A. Apostolov, I. Apostolova, and J. Wesselinowa, "Theory of phonon properties in doped and undoped CuO nanoparticles," *Physics Letters A*, vol. 376, no. 33, pp. 2252-2255, 2012.
- [8] M. H. Babu, J. Podder, B. C. Dev, and M. Sharmin, "p to n-type transition with wide blue shift optical band gap of spray synthesized Cd doped CuO thin films for optoelectronic device applications," *Surfaces and interfaces*, vol. 19, p. 100459, 2020.
- [9] N. Kikuchi and K. Tonooka, "Electrical and structural properties of Ni-doped Cu₂O films prepared by pulsed laser deposition," *Thin Solid Films*, vol. 486, no. 1-2, pp. 33-37, 2005.
- [10] İ. Y. Erdoğan and Ö. Güllü, "Optical and structural properties of CuO nanofilm: its diode application," *Journal of Alloys and Compounds*, vol. 492, no. 1-2, pp. 378-383, 2010.
- [11] M. Al-Kuhaili, "Characterization of copper oxide thin films deposited by the thermal evaporation of cuprous oxide (Cu₂O)," *Vacuum*, vol. 82, no. 6, pp. 623-629, 2008.
- [12] S. Baturay *et al.*, "Modification of electrical and optical properties of CuO thin films by Ni doping," *Journal of Sol-Gel Science and Technology*, vol. 78, no. 2, pp. 422-429, 2016.
- [13] P. Sahoo, S. Dhara, S. Dash, S. Amirthapandian, A. K. Prasad, and A. Tyagi, "Room temperature H₂ sensing using functionalized GaN nanotubes with ultra low activation energy," *International journal of hydrogen energy*, vol. 38, no. 8, pp. 3513-3520, 2013.
- [14] A. Pramothkumar, N. Senthilkumar, R. M. Jenila, M. Durairaj, T. S. Girisun, and I. V. Potheher, "A study on the electrical, magnetic and optical limiting behaviour of Pure and Cd-Fe co-doped CuO NPs," *Journal of Alloys and Compounds*, vol. 878, p. 160332, 2021.
- [15] T. H. Tran *et al.*, "Effect of annealing temperature on morphology and structure of CuO nanowires grown by thermal oxidation method," *Journal of Crystal Growth*, vol. 505, pp. 33-37, 2019.
- [16] R. Arunadevi, B. Kavitha, M. Rajarajan, A. Suganthi, and A. Jeyamurugan, "Investigation of the drastic improvement of photocatalytic degradation of Congo red by monoclinic Cd, Ba-CuO nanoparticles and its antimicrobial activities," *Surfaces and Interfaces*, vol. 10, pp. 32-44, 2018.
- [17] S. Masudy-Panah, K. Radhakrishnan, H. R. Tan, R. Yi, T. I. Wong, and G. K. Dalapati, "Titanium doped cupric oxide for photovoltaic application," *Solar Energy Materials and Solar Cells*, vol. 140, pp. 266-274, 2015.
- [18] A. Tombak, M. Benhaliliba, Y. Ocak, and T. Kiliçoglu, "The novel transparent sputtered p-type CuO thin films and Ag/p-CuO/n-Si Schottky diode applications," *Results in Physics*, vol. 5, pp. 314-321, 2015.
- [19] R. Pandya, H. Patel, N. Shah, P. Solanki, Y. Jani, and M. Keshvani, "Substitutional effect of copper replacement by cadmium on structural, microstructural and electrical properties of Cu_{1-x}Cd_xO oxides," *Materials Today Communications*, vol. 25, p. 101458, 2020.
- [20] M. M. H. Babu, J. Podder, R. R. Tofa, and L. Ali, "Effect of Co doping in tailoring the crystallite size, surface morphology and optical band gap of CuO thin films prepared via thermal spray pyrolysis," *Surfaces and Interfaces*, vol. 25, p. 101269, 2021.